Journal of Quantitative Spectroscopy & Radiative Transfer 112 (2011) 2068–2078

Contents lists available at ScienceDirect

Journal of Quantitative Spectroscopy & Radiative Transfer

journal homepage: www.elsevier.com/locate/jqsrt

Review

Numerically exact computer simulations of light scattering by densely packed, random particulate media

Janna M. Dlugach [a], Michael I. Mishchenko [b,*], Li Liu [b], Daniel W. Mackowski [c]

[a] Main Astronomical Observatory of the National Academy of Sciences of Ukraine, 27 Zabolotny Street, 03680 Kyiv, Ukraine
[b] NASA Goddard Institute for Space Studies, 2880 Broadway, NY 10025, USA
[c] Department of Mechanical Engineering, Auburn University, AL 36849, USA

ARTICLE INFO

Available online 20 February 2011

Keywords:
Maxwell equations
Electromagnetic scattering
Opposition effects
Coherent backscattering
Radiative transfer

ABSTRACT

Direct computer simulations of electromagnetic scattering by discrete random media have become an active area of research. In this progress review, we summarize and analyze our main results obtained by means of numerically exact computer solutions of the macroscopic Maxwell equations. We consider finite scattering volumes with size parameters in the range [20,60], composed of varying numbers of randomly distributed particles with different refractive indices. The main objective of our analysis is to examine whether all backscattering effects predicted by the low-density theory of coherent backscattering (CB) also take place in the case of densely packed media. Based on our extensive numerical data we arrive at the following conclusions: (i) all backscattering effects predicted by the asymptotic theory of CB can also take place in the case of densely packed media; (ii) in the case of very large particle packing density, scattering characteristics of discrete random media can exhibit behavior not predicted by the low-density theories of CB and radiative transfer; (iii) increasing the absorptivity of the constituent particles can either enhance or suppress typical manifestations of CB depending on the particle packing density and the real part of the refractive index. Our numerical data strongly suggest that spectacular backscattering effects identified in laboratory experiments and observed for a class of high-albedo Solar System objects are caused by CB.

Published by Elsevier Ltd.

Contents

1. Introduction

Two optical phenomena, viz., the sharp and narrow brightness opposition effect (BOE) and the polarization

* Corresponding author. Tel.: +1 212 678 5590; fax: +1 212 678 5622.
E-mail addresses: mmishchenko@giss.nasa.gov, crmim2@gmail.com (M.I. Mishchenko).

0022-4073/$ - see front matter Published by Elsevier Ltd.
doi:10.1016/j.jqsrt.2011.02.009

opposition effect (POE, otherwise known as the azimuthal asymmetry of the polarized backscattering cone), have been observed for a class of high-albedo Solar System bodies (see, e.g., Refs. [1–4] and references therein) as well as identified in laboratory measurements for particulate media with large values of the volume packing density [5–10]. The BOE manifests itself as a spike-like intensity peak centered at exactly the backscattering direction, while the POE is observed in the form of a sharp asymmetric negative-polarization feature with a minimum at a phase angle comparable to the angular semi-width of the BOE. Both features have been attributed to the effect of coherent backscattering (CB) in particulate media (see, e.g., Refs. [4,11] and references therein). It should be kept in mind, however, that the interference concept of CB is strictly applicable only in the asymptotic limit of infinitesimally small packing density [11–14]. Therefore, one faces a fundamental question of whether the effect of CB can also account for the specific backscattering phenomena observed in the case of densely packed media.

A definitive answer to this question can only be obtained using extensive numerically exact computations of light scattering characteristics of media composed of varying numbers of randomly positioned particles [13,14]. The steadily increasing power of computers and the availability of efficient numerical techniques have recently facilitated the emergence of an accurate quantitative approach to solving this complex problem based on direct computer solutions of the macroscopic Maxwell equations [15–43]. This approach can be used, in particular, to assess predictions and conditions of applicability of different approximate theories and idealized physical concepts [13,14,32,38].

In this progress review, we analyze the behavior of backscattering characteristics of macroscopic volumes of discrete random medium with varying packing density using numerically exact data obtained recently by directly solving the macroscopic Maxwell equations. The main objective is to examine whether the optical effects predicted by the low-density theory of CB also take place in the case of densely packed media. We provide a summary of the main results obtained in our recent publications as well as discuss new inferences based on numerical results for particulate volumes with very high packing densities or composed of absorbing constituent particles.

2. Theory

The effect of CB is a fascinating optical phenomenon, which can survive essentially any degree of randomness of particle positions [11,12]. The interference origin of CB has its roots in the far-field version of the Foldy–Lax equations [11] and is explained schematically in Fig. 1a, which shows a random multi-particle group illuminated by a plane electromagnetic wave incident in the direction of the unit vector $\hat{\mathbf{n}}_{ill}$ and observed from a very large distance. If the direction of observation, given by the unit vector $\hat{\mathbf{n}}_{obs}$, is far from the exact backscattering direction defined by the unit vector $-\hat{\mathbf{n}}_{ill}$ then the average effect of the interference of a pair of conjugate scattered waves going through a chain of n particles in opposite directions is zero, owing to the randomness of particle positions. Consequently, the detector of electromagnetic energy measures some average, incoherent (or diffuse) intensity. However, when the phase angle α (i.e., the angle between the vectors $\hat{\mathbf{n}}_{obs}$ and $-\hat{\mathbf{n}}_{ill}$) is zero, the phase difference between the conjugate paths involving any chain of particles vanishes, and the interference is always constructive.

The most well-known manifestation of the interference origin of CB is the BOE in the form of a narrow peak of intensity centered at $\alpha=0^\circ$ (see, e.g., Refs. [6–8]). On the other hand, the physical explanation of the interference origin of the POE is more complicated [44–46] and is given in Fig. 1b.[1] Particles 1–4 lie in a plane normal to the illumination direction and are assumed to have sizes much smaller than the wavelength. Particles 1 and 2 lie in the scattering plane (i.e., the plane containing both unit vectors $\hat{\mathbf{n}}_{ill}$ and $\hat{\mathbf{n}}_{obs}$, shown by yellow), while the line through particles 3 and 4 is normal to this plane. If the incident light is unpolarized then both magenta trajectories cause scattered light polarized negatively with respect to the scattering plane, whereas both blue trajectories cause positively polarized scattered light. The phase difference between the conjugate magenta trajectories is always zero, while that between the blue trajectories is zero if $\alpha=0^\circ$ and oscillates rapidly with increasing α. Therefore, on average, CB enhances the contribution of the negatively polarizing scattering trajectories over a wider range of phase angles than that of the positively polarizing trajectories. The result is a negative-polarization minimum at a small phase angle comparable to the angular semi-width of the coherent BOE [44,49]. The fact that only specific particle configurations contribute to the POE often makes the latter less pronounced than the BOE.

Fig. 2 shows the results of computations performed in [49] by using the asymptotic low-density theory of CB in the case of a semi-infinite homogeneous slab composed of sparsely distributed non-absorbing Rayleigh scatterers [50,51]. One can clearly see the most obvious manifestations of the effect of CB such as a narrow peak of intensity centered at zero phase angle and a sharp asymmetric minimum of negative polarization at a small phase angle comparable to the angular semi-width of the coherent intensity peak.

The interference concept of CB explicitly relies on assigning a phase to the wave scattered by a particle. This implies that particles must be located at large distances from each other, in the so-called far-field zone (see, e.g., Refs. [11,12]). However, as we have stressed in Section 1, many laboratory measurements for densely packed particle suspensions and particulate surfaces as

[1] It is worth clarifying that this optical phenomenon was introduced in Refs. [47,48] as a way of explaining the wide, nearly parabolic negative branch in the polarization phase curves exhibited by the majority of atmosphereless Solar System bodies [4]. However, it was shown in Refs. [44,49] that CB results in the highly asymmetric spike-like POE rather than in the much more ubiquitous, nearly symmetric negative-polarization branch (NPB). The very term "POE" was introduced in Ref. [44].

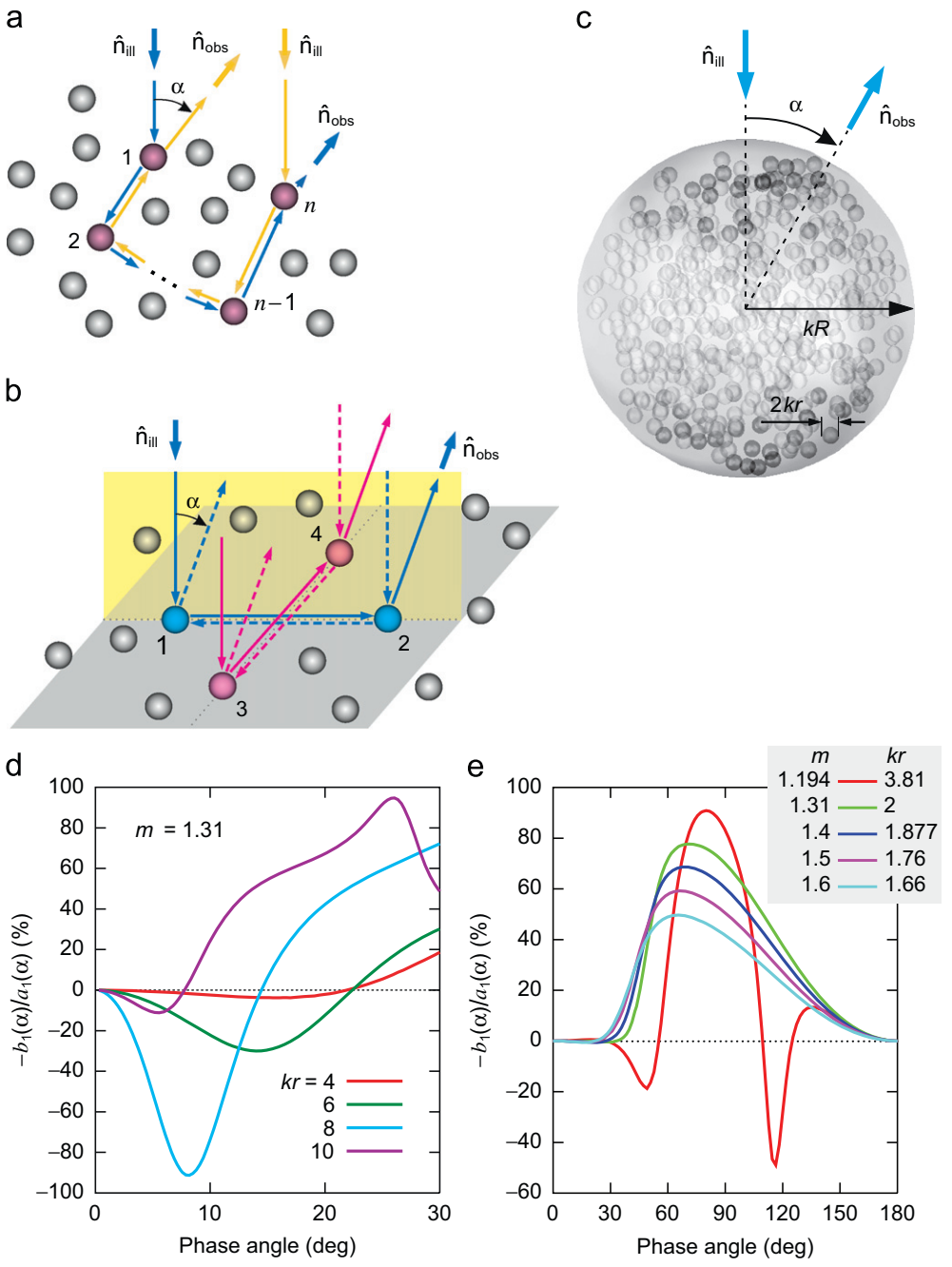

Fig. 1. (a) Schematic demonstration of the interference origin of the CB effect. (b) Schematic explanation of the CB origin of the POE. (c) Scattering by a macroscopic spherical volume randomly filled with small spherical particles. (d) Polarization of scattered light for a single ice sphere with different values of the size parameter *kr*. (e) Polarization of scattered light for a single sphere with several combinations of the refractive index *m* and size parameter *kr*.

well as observations performed for a class of high-albedo Solar System bodies appear to exhibit the unique features predicted by the low-density theory of CB. Therefore, it is necessary to perform numerically exact computations of light scattering based on a direct computer solution of the macroscopic Maxwell equations in order to examine the applicability of the sparse-medium concept of CB to densely packed media in which particles are often in direct contact with each other instead of being separated by large distances.

3. Numerically exact computer modeling

Our model of random particulate medium is a spherical volume of radius R filled with N identical non-overlapping spherical particles of radius r (see Fig. 1c).

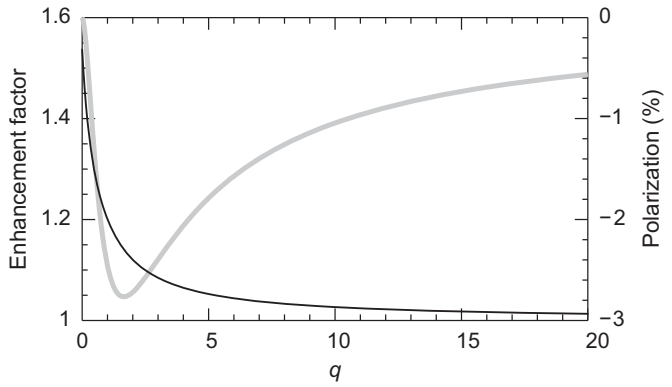

Fig. 2. Angular profiles of the enhancement factor (black curve) and the degree of linear polarization (gray curve) for a semi-infinite homogeneous slab composed of sparsely distributed non-absorbing Rayleigh scatters and illuminated by normally incident unpolarized light [49]. The enhancement factor is defined as the ratio of the total scattered intensity to that of the incoherent (diffuse) background. The angular parameter q is defined as the product of the phase angle, the wave number, and the mean free path of light in the scattering medium.

The size parameter of the volume is kR, and the particle size parameter is kr, where k is the wave number. To model statistically random and uniform particle positions within the spherical volume consistent with the fundamental assumption of ergodicity [11], we follow the approach pioneered in Ref. [22]. Specifically, we use one realization of an N-particle group generated randomly according to the procedure described in [52], and then average all optical observables of interest over the uniform orientation distribution of this configuration with respect to the laboratory coordinate system. Although the mutual positions of the N particles with respect to each other remain the same, they are sufficiently "random" to begin with. Therefore, this simple approach yields, in effect, an infinite continuous set of random realizations of the scattering volume while enabling one to use the efficient orientation averaging technique afforded by the superposition T-matrix method (STMM) [53–55]. The STMM represents a direct computer solver of the macroscopic Maxwell equations for an arbitrary multisphere configuration [56]. Within the range of its numerical convergence, the corresponding public-domain T-matrix computer code [57] yields results with a guaranteed accuracy, which makes it numerically exact.

It is obvious that by its very construct, this scattering model cannot be expected to reproduce exactly the infinite diversity of morphologies of particulate media encountered in laboratory and natural conditions. However, it proves to be sufficiently representative to permit a robust and instructive analysis of the effects of packing density on multiple scattering of light by discrete random media.

It is further assumed that the statistically random particulate volume is illuminated by a parallel quasi-monochromatic beam of light propagating in the direction of the unit vector $\hat{\mathbf{n}}_{ill}$ (Fig. 1c). The observer is located in the far-field zone of the entire spherical volume in the direction of the unit vector $\hat{\mathbf{n}}_{obs}$. Since all scattering and absorption properties of the particulate volume are averaged uniformly over all orientations of the N-particle group, they depend only on the phase angle α provided that the scattering plane is used for defining the Stokes parameters of the incident and scattered light. The far-field transformation of the Stokes parameters I, Q, U, and V upon scattering by the entire particulate volume is then formulated in terms of the 4×4 real-valued Stokes scattering matrix [11,56,58]

$$\begin{bmatrix} I^{sca} \\ Q^{sca} \\ U^{sca} \\ V^{sca} \end{bmatrix} \propto \begin{bmatrix} a_1(\alpha) & b_1(\alpha) & 0 & 0 \\ b_1(\alpha) & a_2(\alpha) & 0 & 0 \\ 0 & 0 & a_3(\alpha) & b_2(\alpha) \\ 0 & 0 & -b_2(\alpha) & a_4(\alpha) \end{bmatrix} \begin{bmatrix} I^{inc} \\ Q^{inc} \\ U^{inc} \\ V^{inc} \end{bmatrix}. \tag{1}$$

In theory [56,59], the off-block diagonal elements of the scattering matrix would be zero only if the primordial N-sphere configuration had a plane of symmetry. We found, however, that in all the cases considered below the magnitude of the minor matrix elements denoted in Eq. (1) by zeros is much smaller than that of the major elements. In other words, the zeros denote the scattering matrix elements negligibly small (in the absolute sense) relative to the other elements at the same scattering angles. The (1, 1) element $a_1(\alpha)$, called the phase function, is normalized according to the standard integral condition

$$\frac{1}{2}\int_0^{\pi} a_1(\alpha)\sin\alpha\, d\alpha = 1. \tag{2}$$

The elements of the scattering matrix can be used to define conventional optical observables corresponding to different types of polarization state of the incident radiation used in remote-sensing, *in situ*, and laboratory particle characterization (see, e.g., Refs. [60–66] and references therein). Specifically, if the incident light is unpolarized then the phase function characterizes the angular distribution of the far-field scattered intensity, while the ratio $-b_1/a_1$ gives the corresponding degree of linear polarization. If the incident radiation is polarized linearly in the scattering plane (i.e., $Q^{inc}=I^{inc}$, $U^{inc}=V^{inc}=0$) then the linear polarization ratio μ_L is defined as the ratio of the cross-polarized and co-polarized components of the scattered intensity

$$\mu_L(\alpha) = \frac{a_1(\alpha)-a_2(\alpha)}{a_1(\alpha)+2b_1(\alpha)+a_2(\alpha)}. \tag{3}$$

If the incident radiation is polarized circularly in the counterclockwise direction when looking in the direction of propagation (i.e., $V^{inc}=I^{inc}$, $Q^{inc}=U^{inc}=0$), then the circular polarization ratio μ_C is defined as the ratio of the same-helicity and opposite-helicity components of the scattered intensity

$$\mu_C(\alpha)=\frac{a_1(\alpha)+a_4(\alpha)}{a_1(\alpha)-a_4(\alpha)}. \quad (4)$$

By using the numerically exact computer solver of the macroscopic Maxwell equations, we have performed extensive computations of the scattering characteristics of particulate volumes with size parameters kR in the range from 20 up to 60, filled with non-absorbing spherical particles with real-valued refractive indices $m=1.194$ (representing latex in water), 1.31 (representing liquid water and water ice at visible wavelengths), and 1.4, 1.5, 1.6 (representing different mineral substances) [33,34]. Depending on kR, the number of monomers N varies from 1 up to 900 (for $m=1.31$ and $kR=30$). Also we present some numerical data for absorbing particles with $m_R=Re(m)=1.31$ and 1.5 and $m_I=Im(m)=0.01$, 0.1, and 0.3.

The corresponding values of the packing density depend on the way the particle volume fraction is defined. If R is the radius of the sphere enclosing all constituent particles completely then the packing density ρ is defined as the ratio of the cumulative volume of the constituent particles to the total enclosed volume: $\rho=Nr^3/R^3$. However, this definition underestimates the actual packing density inside the scattering medium since the constituent particles are not allowed to cross the bounding sphere (Fig. 1c). Therefore, in what follows we define the packing density as $\tilde{\rho}=Nr^3/(R-r)^3$, where $R-r$ is the radius of the sphere enclosing all constituent-particle centers.

It should be kept in mind that a direct computer modeling of the POE can be quite problematic because the degree of linear polarization of light singly scattered by a constituent particle (for unpolarized incident light) often has a negative branch at small phase angles [67,68]. As an example, Fig. 1d shows the computed values of polarization for an ice sphere with the refractive index $m=1.31$ and several values of the size parameter kr. We see that in all cases, the computed polarization has a negative branch in the range of phase angles $[0^\circ, 20^\circ]$. This fact makes it non-trivial to distinguish between the singly and multiply scattered negative-polarization contributions in a direct numerical solution of the Maxwell equations. In order to eliminate this uncertainty, for each value of the refractive index studied we have selected a size parameter value yielding a single-scattering polarization contribution with a wide horizontal "shelf" of near-zero values at small phase angles. The resulting {refractive index, size parameter} pairs and the corresponding single-scattering polarization curves are shown in Fig. 1e. One can clearly identify indeed a horizontal shelf of near-zero values of polarization in the range of phase angles $0^\circ \le \alpha \le 30^\circ$, which makes any multiple-scattering polarization contribution easily discernable and quantifiable. Note that this approach was proposed in our recent publications [33,34] and was used to obtain the first ever numerically exact display of the entire suite of backscattering optical effects implied by the asymptotic low-density theory of CB.

4. Numerical results and discussion

In this section, we present and analyze numerical results obtained for both non-absorbing and absorbing constituent particles.

4.1. Scattering volumes filled with non-absorbing particles

Figs. 3 and 4 provide a representative subset of our extensive numerical results computed for non-absorbing constituent particles. In some cases, we also show the results computed for a single isolated spherical particle. Since we are interested in the backscattering behavior of all optical observables, we consider only the range of phase angles $0^\circ \le \alpha \le 30^\circ$.

Fig. 3a depicts the results of computations for $m=1.31$, $kR=40$, $kr=2$, and packing densities $\tilde{\rho}$ varying between 1.5% ($N=100$) and 11.7% ($N=800$). For reference, we also show the corresponding singe-particle data. We see that these numerically exact results are in perfect qualitative agreement with the predictions of the low-density theory of CB. Indeed,

1. The normalized scattered intensity $a_1(\alpha)/a_1(0)$ exhibits backscattering peaks rapidly developing with N. The angular widths of these peaks are approximately the same.
2. In the phase-angle range $0^\circ \le \alpha \le 30^\circ$, the degree of linear polarization $-b_1(\alpha)/a_1(\alpha)$ is equal to zero for $N=1$ but rapidly develops a pronounced minimum with growing N caused by the increasing amount of multiple scattering. The phase angle of minimal polarization, α_{min}, is virtually independent on N and is comparable to the angular semi-width of the coherent BOE. Furthermore, the angular shape of the negative-polarization minima is asymmetric, with α_{min} being significantly closer to zero than to the phase angle at which polarization switches sign from negative to positive (the so-called inversion angle). As such, the polarization minima in Fig. 3a have the same basic morphology as the POE predicted by the low-density theory of CB, although the polarization curve in Fig. 2 is based on the assumption of a phase-angle-independent ladder contribution and, as a consequence, shows no inversion.
3. The backscattering peaks in the linear and circular polarization-ratio curves are absent in the case of a single particle but develop and rapidly grow with increasing N. The angular widths of all these peaks are approximately the same and independent of N.

In order to analyze the dependence of these optical observables on the volume size parameter kR, we present in Fig. 3b the computational data obtained for $m=1.31$, $N=800$, and $kR=30$, 40, and 60. It is seen that the angular

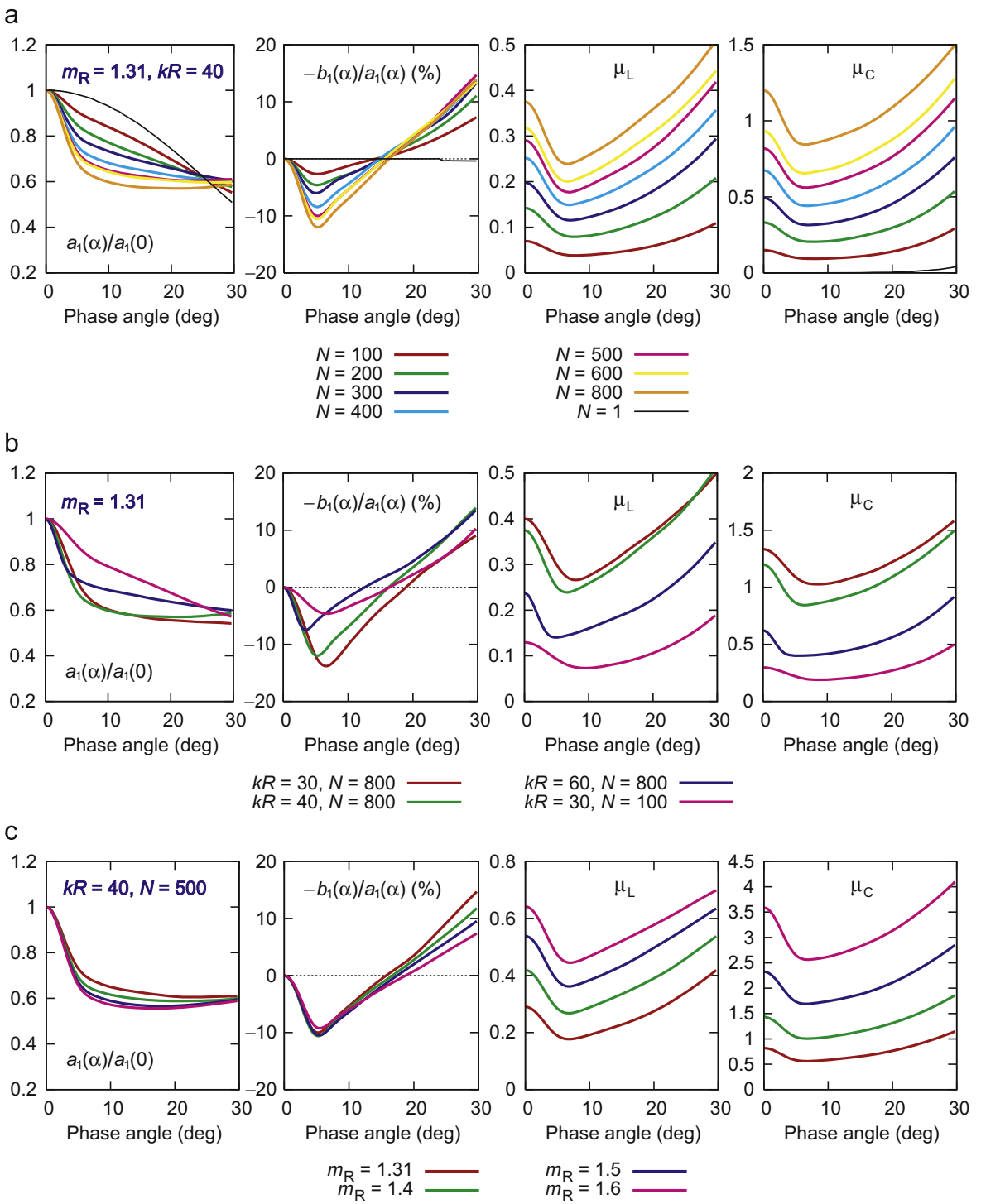

Fig. 3. (a) Backscattering characteristics of a kR=40 scattering volume randomly filled with a number N of kr=2 spherical particles. The packing density varies between $\tilde{\rho}=1.5\%$ (N=100) and $\tilde{\rho}=11.7\%$ (N=800). The particle refractive index is fixed at m=1.31. (b) Backscattering characteristics of particulate volumes with size parameters in the range $30 \le kR \le 60$. The particle refractive index is fixed at m=1.31 and their size parameter is fixed at kr=2. (c) Backscattering characteristics of a particulate volume with kR=40 and N=500. The particle refractive index m varies from 1.31 to 1.6. The respective values of the particle size parameter are listed in the legend of Fig. 1e. The packing density $\tilde{\rho}$ varies between 7.3% (m=1.31) and 4.1% (m=1.6).

widths of all the backscattering peaks and the angles of minimal polarization decrease with increasing kR approximately as $1/kR$.

Also shown for comparison are the results for kR=30 and N=100. In this latter case, the particle packing density $\tilde{\rho}$ is approximately the same as in the case of kR=60 and

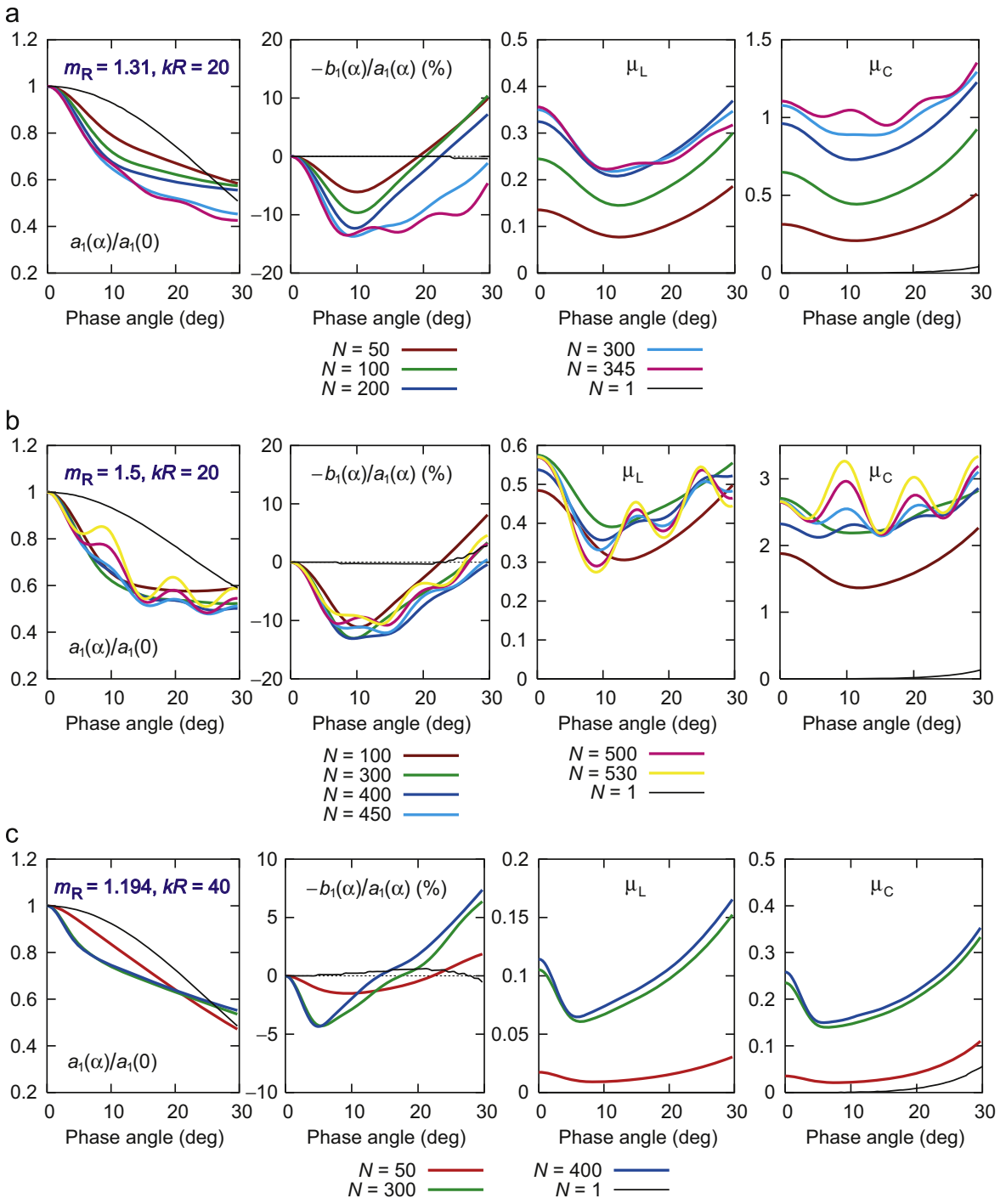

Fig. 4. Optical characteristics of kR=20 (panels a and b) and 40 (panel c) scattering volumes randomly filled with different numbers N of spherical particles with (a) m=1.31, (b) m=1.5, and (c) m=1.194. The packing density $\tilde{\rho}$ in panel (c) varies between 5.8% (N=50) and 46.7% (N=400).

N=800 (3.6% and 3.3%, respectively). It is seen that for the same volume fraction, the backscattering enhancement in the intensity and polarization ratios as well as the depth of the negative-polarization branch increase with increasing kR, while their angular widths decrease approximately by a factor of two.

In Fig. 3c, we show the results for the volume size parameter kR=40, the number of monomers N=500, and refractive indices m=1.31, 1.4, 1.5, and 1.6 (the corresponding values of the particle size parameter kr are given in Fig. 1e). One can see very similar opposition effects for all four refractive-index values, which illustrates the

universal interference nature of CB. Quite remarkably, the angular widths of all the backscattering peaks are virtually independent of the particle refractive index, while the negative-polarization features are almost identical.

From Fig. 3, we can conclude that all curves of normalized scattered intensity $a_1(\alpha)/a_1(0)$ and linear polarization $-b_1(\alpha)/a_1(\alpha)$ for $N>1$ reveal the BOE and the POE, respectively. Indeed, all traits in the behavior of the normalized intensity peaks and the polarization minima testify to their interference multiple-scattering origin. Specifically, the intensity peaks and polarization minima are absent in the single-particle curves but are present when $N>1$. The angular semi-width of the normalized intensity peak is comparable to the phase angle of minimal polarization α_{min}. Both of them are independent of N and m and are inversely proportional to the value of the volume size parameter kR. Furthermore, the polarization minima become increasingly asymmetric with increasing kR and approach the classical angular profile shown by the gray curve in Fig. 2. Note, that the linear and circular polarization-ratio curves are even more indicative of their multiple-scattering origin since they are absent completely for a single spherical particle. For a fixed kR, the angular widths of the backscattering peaks in the μ_L and μ_C curves are approximately the same and are independent of the number of particles and their refractive index. Furthermore, they scale as $1/kR$, thereby corroborating their CB nature.

The effect of increasing the number of particles N in a volume can be expected to be twofold. Initially it stimulates multiple scattering and thus enhances the classical manifestations of diffuse radiative transfer (RT) and CB. Eventually, however, it can cause changes in the scattering patterns not implied by the low-packing-density theories of RT and CB. One should, therefore, expect that the RT and CB interpretation of the numerically exact T-matrix results must become inadequate when $\tilde{\rho}$ becomes sufficiently large.

In order to analyze the effects of increasing N, we present the STMM results for kR=20, m=1.31, kr=2, and N varying from 50 ($\tilde{\rho}\sim 7\%$) up to 345 ($\tilde{\rho}\sim 47\%$) (Fig. 4a), as well as for m_R=1.5, kr=1.76, and N varying from 100 ($\tilde{\rho}\sim 9\%$) up to 530 ($\tilde{\rho}\sim 48\%$) (Fig. 4b). We see that, indeed, starting from N=300 ($\tilde{\rho}\sim 41\%$) the curves in Fig. 4a develop high-frequency interference ripples typical of a single spherical particle with a size substantially greater than the wavelength [56]. Similar behavior is seen in Fig. 4b starting from N=400 ($\tilde{\rho}\sim 35\%$). Obviously, this behavior is not predicted by the low-density theories of RT and CB. Nevertheless, the results of our computations do demonstrate that the predictions of these asymptotic theories can survive substantial volume packing densities typical of particulate surfaces and particle suspensions.

It should be noted that the dense-packing behavior of the backscattering characteristics considered is not universal, as the data shown in Fig. 4c demonstrate. Indeed, the STMM results for kR=40, m=1.194, kr=3.81 (cf. Fig. 1e), and N varying from 50 ($\tilde{\rho}\sim 6\%$) up to 400 ($\tilde{\rho}\sim 47\%$) exhibit the "standard" CB behavior despite packing densities reaching 47%. Apparently, this behavior is somehow related to the optical "softness" of the constituent particles.

4.2. Scattering media composed of absorbing particles

It is well known that absorption can diminish various manifestations of multiple scattering significantly (see, e.g., [11,25]). Therefore, it is important to verify whether the CB multiple-scattering interpretation of the backscattering features identified for scattering media composed of non-absorbing particles is consistent with the way in which these features should be expected to change upon increasing absorption. Note that earlier in [25], using the results of computations for m_R=1.32 and $\tilde{\rho}=22\%$, it was concluded that increasing absorption suppresses such optical effects as BOE and depolarization.

Some of the results of our extensive computations are presented in Fig. 5. The computations have been performed for a kR=30 scattering volume composed of spherical particles with m_R=1.31 (Fig. 5a), 1.5 (Fig. 5b), and m_I=0, 0.01, 0.1, and 0.3. The values of the particle size parameter were adopted to be the same as in the case of m_I=0 (i.e., kr=2 for m_R=1.31 and 1.76 for m_R=1.5). In the case of m_R=1.31, the number of constituent particles N was varied from 100 up to 400, which corresponds to the variation of the packing density $\tilde{\rho}$ from 3.6% up to 14.6%; for m_R=1.5, N was varied from 100 ($\tilde{\rho}=2.4\%$) up to 600 ($\tilde{\rho}=14.5\%$).

Fig. 5a presents the results for the real part of the refractive index m_R=1.31. We see that:

1. In the range of phase angles $0^\circ<\alpha<10^\circ$, the amplitude of the backscattering peak in the normalized scattered intensity $a_1(\alpha)/a_1(0)$ caused by CB decreases with increasing absorption.
2. The depth of the negative branch in the curves of linear polarization $-b_1(\alpha)/a_1(\alpha)$ decreases monotonously with increasing m_I; when m_I=0.3, the polarization curve changes its shape.
3. Increasing absorption diminishes progressively the values of the linear and circular polarization ratios; when m_I=0.3, both ratios become very small.

All these results can easily be interpreted in terms of the decreasing contribution of multiple scattering with increasing absorption. It is known that absorption terminates long scattering paths and thereby can be expected to reduce the range of phase angles affected by CB [69]. This can be seen indeed in our results which exhibit, in particular, a decrease in the width of the BOE and the phase angle of minimal polarization α_{min} with decreasing m_I.

Somewhat different results are obtained in the case of the real part of the refractive index m_R=1.5 and the number of constituent particles N=100 (Fig. 5b). In this case:

1. Increasing the imaginary part m_I from 0 up to 0.1 results in a stronger backscattering intensity peak $a_1(\alpha)/a_1(0)$. Furthermore, the backscattering enhancement is still quite pronounced when m_I=0.3, which is indicative of a significant residual contribution of multiple scattering even in the case of such strong absorption.
2. The behavior of the depth of the negative-polarization branch with increasing absorption is not monotonous: it first increases and then decreases.

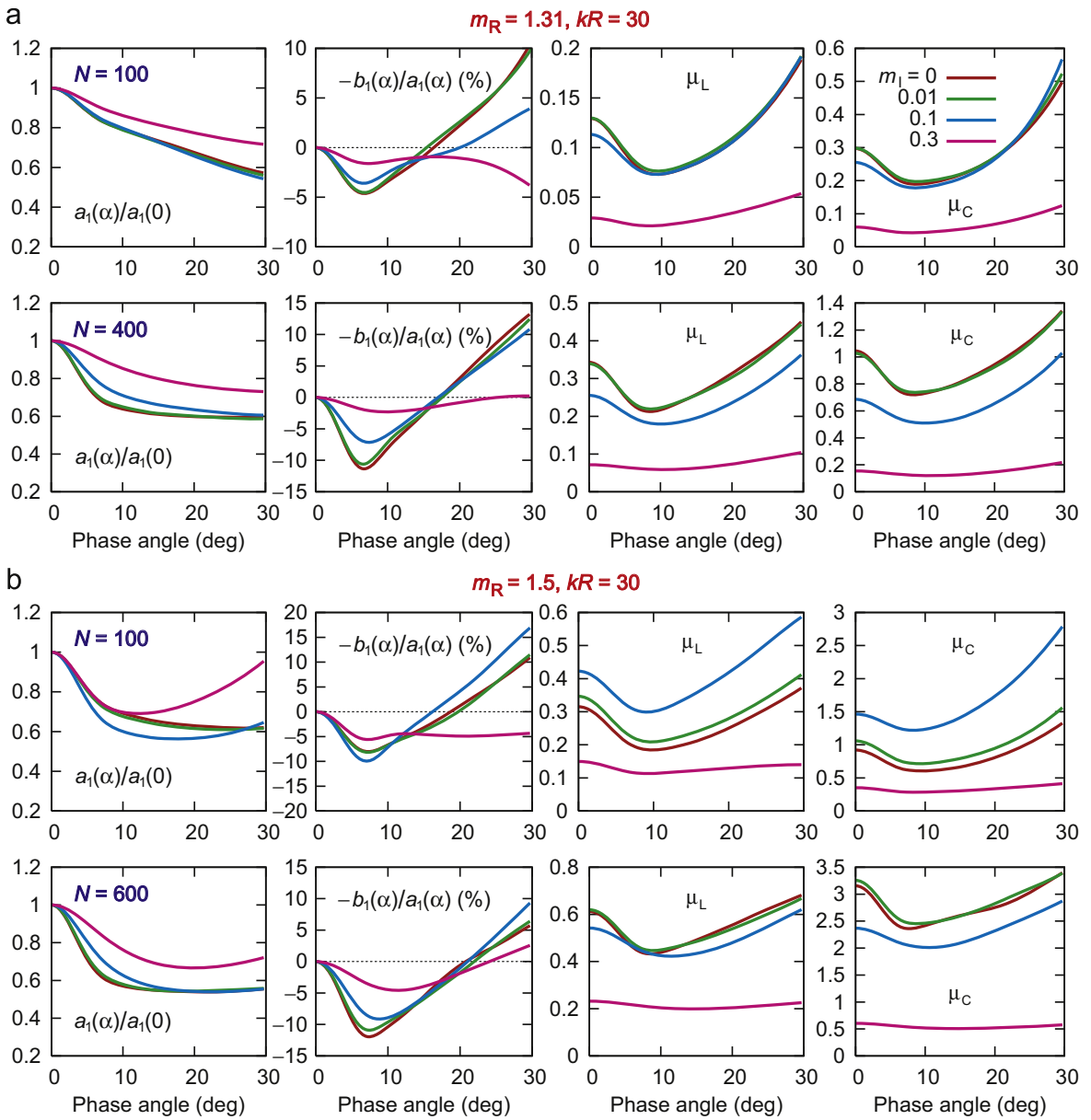

Fig. 5. Scattering characteristics of a kR=30 scattering volume randomly filled with N identical spherical particles. (a) m_R=1.31, N=100 (upper row), and N=400 (lower row); (b) m_R=1.5, N=100 (upper row), and N=600 (lower raw). The imaginary part of the refractive index varies in the range $0 \le m_I \le 0.3$ according to the color legend in the top right-hand diagram.

3. The polarization ratios μ_L and μ_C also demonstrate a significant growth as m_I increases from 0 up to 0.1, followed by a precipitous decrease. At the same time the widths of the backscattering peaks hardly change.

However, in the case of m_R=1.5 and N=600, we see a more monotonous decrease of all the manifestations of the effect of CB with increasing absorption.

Thus, we have to conclude that increasing absorption can either enhance or suppress manifestations of the CB effect depending on the particle packing density and the real part of the refractive index. This is not surprising, since increasing m_I changes not only the absorption properties of the constituent particles but also their scattering (including polarization) properties.

5. Concluding remarks

It must be emphasized once again that our model of a multi-particle scattering volume cannot be expected to reproduce exactly the diverse complex morphologies of particulate media encountered in laboratory and natural conditions. As noted above, the interference base for a finite scattering volume is controlled by its size parameter kR, whereas that for an optically thick, non-absorbing or weakly absorbing layer is controlled by the transport

mean free path [12]. The latter can be much greater than the kR values used in our computations and thereby yield much narrower opposition effects. However, our model has proved to be remarkably robust and permits a thorough qualitative and semi-quantitative analysis of the effects of packing density on multiple light scattering in discrete random media. The critical advantages of the direct computer solution of the Maxwell equations is that it yields numerically exact results, does not involve the simplifying yet questionable assumption of a small packing density, and allows the researcher to vary all physical parameters of the scattering medium one a time [13,14]. This allows one to trace the onset of multiple scattering as the particle number N deviates from one, the evolution of the various manifestations of CB with increasing N, and the eventual onset of packing-density effects [70,71] distorting substantially the angular profiles of the BOE, POE, and polarization ratios with respect to the profiles predicted by the asymptotic low-density theory of CB.

On the basis of the results of our extensive numerically exact computer simulations [20,22,25,31,33,34], we arrive at the following conclusions:

1. All backscattering effects predicted by the low-density theory of CB can also take place in the case of a densely packed medium. The relatively small optical diameters of the particulate volumes considered cause the angular widths of the BOE and POE to scale as $(kR)^{-1}$, in agreement with the interference concept of CB. Computations for significantly larger optical diameters will be needed to reach the $(k\times$transport mean free path$)^{-1}$ scaling.
2. Increasing absorptivity of the constituent particles can either enhance or suppress classical manifestations of the CB effect depending on the particle packing density and the real part of the refractive index. This duality illustrates again the extreme complexity of the effects of multiple scattering in many-particle groups (see, e.g., Ref. [46] where it is shown that absorbing Rayleigh scatters can yield greater enhancement factors and deeper negative-polarization minima than non-absorbing Rayleigh scatters).
3. In the case of very large values of the particle packing density, the scattering characteristics of the particulate volume start to exhibit behavior not predicted by the low-density theories of CB and RT. Nevertheless, the direct computer solutions of the Maxwell equations do demonstrate that the classical low-density predictions can survive (at least in a qualitative and even semi-quantitative sense) volume packing densities typical of particle suspensions and particulate surfaces encountered in natural and man-made conditions.

Furthermore, the accumulated body of evidence supports the conclusion that CB is the likely cause of the uniquely narrow BOE and POE observed for a class of high-albedo Solar System objects [2–4]. Another important implication is that the azimuthal asymmetry of the polarized backscattering cone and the POE observed in the laboratory for densely packed particulate media [5,9,10] are indeed caused by the effect of CB.

Finally, our numerically exact results pose a fundamental question as to why the various manifestations of CB are so remarkably immune to packing density. The definite qualitative answer to this question may not be immediately obvious. However, one may speculate that even in densely packed discrete random media, the partial multiply scattered wavelets that involve widely separated particles still provide a significant cumulative contribution to the total scattered signal and thereby make the classical multiple-scattering and CB features quite pronounced.

Acknowledgments

We acknowledge support from the Ukrainian National Academy of Sciences under the Main Astronomical Observatory GRAPE/GPU/GRID computing cluster project. This research was sponsored by the NASA Radiation Sciences Program managed by Hal Maring and by the NASA Glory Mission project.

References

[1] Muinonen K, Piironen J, Shkuratov YuG, et al. Asteroid photometric and polarimetric phase effects. In: Bottke Jr. WF, Cellino A, Paolicchi P, Binzel RP, editors. Asteroids III. Tucson, AZ: University of Arizona Press; 2002. p. 123–38.
[2] Rosenbush V, Kiselev N, Avramchuk V, Mishchenko M. Photometric and polarimetric phenomena exhibited by solar system bodies. In: Videen G, Kocifaj M, editors. Optics of cosmic dust. Dordrecht: Kluwer; 2002. p. 191–224.
[3] Mishchenko MI, Rosenbush VK, Kiselev NN. Weak localization of electromagnetic waves and opposition phenomena exhibited by high-albedo atmosphereless solar system objects. Appl Opt 2006;45:4469–73.
[4] Mishchenko MI, Rosenbush VK, Kiselev NN et al. Polarimetric remote sensing of Solar System objects. Kyiv: Akademperiodyka; 2010, ⟨arXiv:1010.1171⟩.
[5] Lyot B. Recherches sur la polarisation de la lumière des planets et de quelques substances terrestres. Ann Obs Paris Sect Meudon 1929;8:1–161.
[6] Kuga Y, Ishimaru A. Retroreflectance from a dense distribution of spherical particles. J Opt Soc Am A 1984;1:831–5.
[7] van Albada MP, van der Mark MB, Lagendijk J. Observation of weak localization of light in a finite slab: anisotropy effects and light path classification. Phys Rev Lett 1987;58:361–4.
[8] Wolf P, Maret G. Weak localization and coherent backscattering of photons in disordered media. Phys Rev Lett 1985;55:2696–9.
[9] van Albada MP, van der Mark MB, Lagendijk J. Polarization effects in weak localization of light. J Phys D 1988;21:S28–31.
[10] Shkuratov Yu, Ovcharenko A, Zubko E, et al. The opposition effect and negative polarization of structural analogs for planetary regoliths. Icarus 2002;159:396–416.
[11] Mishchenko MI, Travis LD, Lacis AA. In: Multiple scattering of light by particles: radiative transfer and coherent backscattering. Cambridge: Cambridge U. Press; 2006.
[12] Barabanenkov YuN, Kravtsov YuA, Ozrin VD, Saichev AI. Enhanced backscattering in optics. Prog Opt 1991;29:65–197.
[13] Tishkovets VP, Mishchenko MI. Coherent backscattering: conceptions and misconceptions. J Quant Spectrosc Radiat Transfer 2010;111:645–9.
[14] Mishchenko MI, Tishkovets VP, Travis LD, et al. Electromagnetic scattering by a morphologically complex object: fundamental concepts and common misconceptions. J Quant Spectrosc Radiat Transfer 2011;112:671–92.
[15] Mishchenko MI. Coherent backscattering by two-sphere clusters. Opt Lett 1996;21:623–5.
[16] Roux L, Mareschal P, Vukadinovic N, Thibaud J-B, Greffet J-J. Scattering by a slab containing randomly located cylinders: comparison between radiative transfer and electromagnetic simulation. J Opt Soc Am A 2001;18:374–84.

[17] Tseng SH, et al. Exact solution of Maxwell's equations for optical interactions with a macroscopic random medium. Opt Lett 2004;29:1393–5.
[18] Tseng SH, et al. Simulation of enhanced backscattering of light by numerically solving Maxwell's equations without heuristic approximations. Opt Express 2005;13:3666–72.
[19] Tseng SH, Taflove A, Maitland D, Backman V. Pseudospectral time domain simulations of multiple light scattering in three-dimensional macroscopic random media. Radio Sci 2006;41:RS4009.
[20] Mishchenko MI, Liu L. Weak localization of electromagnetic waves by densely packed many-particle groups: exact 3D results. J Quant Spectrosc Radiat Transfer 2007;106:616–21.
[21] Tseng SH, Huang B. Comparing Monte Carlo simulation and pseudospectral time-domain numerical solutions of Maxwell's equations of light scattering by a macroscopic random medium. Appl Phys Lett 2007;91:051114.
[22] Mishchenko MI, Liu L, Mackowski DW, et al. Multiple scattering by random particulate media: exact 3D results. Opt Express 2007;15:2822–36.
[23] Tse KK, Tsang L, Chan CH, Ding KH, Leung KW. Multiple scattering of waves by dense random distributions of sticky particles for applications in microwave scattering by terrestrial snow. Radio Sci 2007;42:RS5001.
[24] Mishchenko MI, Liu L, Videen G. Conditions of applicability of the single-scattering approximation. Opt Express 2007;15:7522–7.
[25] Mishchenko MI, Liu L, Hovenier JW. Effects of absorption on multiple scattering by random particulate media: exact results. Opt Express 2007;15:13182–7.
[26] Penttilä A, Lumme K. Coherent backscattering effects with discrete dipole approximation method. In: Videen G, Mishchenko M, Mengüç MP, Zakharova N, editors. Peer-reviewed abstracts of the tenth conference on electromagnetic and light scattering. Bodrum; 2008. p. 157–60, 〈http://www.giss.nasa.gov/staff/mmishchenko/publications/ELS_10_abstracts.pdf〉.
[27] Mackowski DW, Mishchenko MI. Prediction of thermal emission and exchange among neighboring wavelength-sized spheres. J Heat Transfer 2008;130:112702.
[28] Tseng SH. Optical characteristics of a cluster of closely-packed dielectric spheres. Opt Commun 2008;281:1986–90.
[29] Sukhov A, Haefner D, Dogariu A. Coupled dipole method for modeling optical properties of large-scale random media. Phys Rev E 2008;77:066709.
[30] Okada Y, Kokhanovsky AA. Light scattering and absorption by densely packed groups of spherical particles. J Quant Spectrosc Radiat Transfer 2009;110:902–17.
[31] Mishchenko MI, Liu L. Electromagnetic scattering by densely packed particulate ice at radar wavelengths: exact theoretical results and remote-sensing implications. Appl Opt 2009;48:2421–6.
[32] Voit F, Schäfer J, Kienle A. Light scattering by multiple spheres: comparison between Maxwell theory and radiative-transfer-theory calculations. Opt Lett 2009;34:2593–5.
[33] Mishchenko MI, Dlugach JM, Liu L, et al. Direct solutions of the Maxwell equations explain opposition phenomena observed for high albedo solar system objects. Astrophys J 2009;705:L118–22.
[34] Mishchenko MI, Dlugach JM, Liu L. Azimuthal asymmetry of the coherent backscattering cone: theoretical results. Phys Rev A 2009;80:053824.
[35] Ganesh M, Hawkins SC. A high-order algorithm for multiple electromagnetic scattering in three dimensions. Numer Algor 2009;50:469–510.
[36] Starosta MS, Dunn AK. Far-field superposition method for three-dimensional computation of light scattering from multiple cells. J Biomed Opt 2010;15:055006.
[37] Ding M, Chen K. Numerical investigation on polarization characteristics of coherent enhanced backscattering using SLPSTD. Opt Express 2010;18:27639–49.
[38] Muinonen K, Zubko E. Coherent backscattering by a finite medium of particles. In: Muinonen K, Penttilä A, Lindqvist H, Nousiainen T, Videen G, editors. Electromagnetic and light scattering XII. University of Helsinki: Helsinki; 2010. p. 194–7.
[39] Lee S-C. Wave propagation through a dielectric layer containing densely packed fibers. J Quant Spectrosc Radiat Transfer 2011;112:143–50.
[40] Mackowski DW, Mishchenko MI. Direct simulation of multiple scattering by discrete random media illuminated by Gaussian beams. Phys Rev A 2011;83:013804.
[41] Mishchenko MI, Mackowski DW. Coherent backscattering in the cross-polarized channel. Phys Rev A 2011;83:013829.
[42] Lumme K, Penttilä A. Light scattering by dust particles in the solar system: applications to cometary comae and planetary regoliths. J Quant Spectrosc Radiat Transfer, in press, doi:10.1016/j.jqsrt.2011.01.016.
[43] Penttilä A, Lumme K. Optimal cubature on the sphere and other orientation averaging schemes, J Quant Spectrosc Radiat Transfer, in press, doi:10.1016/j.jqsrt.2011.02.001.
[44] Mishchenko MI. On the nature of the polarization opposition effect exhibited by Saturn's rings. Astrophys J 1993;411:351–61.
[45] Shkuratov YuG, Muinonen K, Bowell E, et al. A critical review of theoretical models of negatively polarized light scattered by atmosphereless solar system bodies. Earth Moon Planets 1994;65:201–46.
[46] Muinonen K. Coherent backscattering of light by complex random media of spherical scatters: numerical solution. Waves Random Media 2004;14:365–88.
[47] Shkuratov YuG. A new mechanism for the negative polarization of light scattered by the solid surfaces of cosmic bodies. Astron Vestnik 1989;23:176–80 in Russian.
[48] Muinonen K. Light scattering by inhomogeneous media: backward enhancement and reversal of linear polarization. PhD dissertation, University of Helsinki; 1990.
[49] Mishchenko MI, Luck J-M, Nieuwenhuizen T. Full angular profile of the coherent polarization opposition effect. J Opt Soc Am A 2000;17:888–91.
[50] Ozrin VD. Exact solution for coherent backscattering of polarized light from a random medium of Rayleigh scatterers. Waves Random Media 1992;2:141–64.
[51] Amic E, Luck JM, Nieuwenhuizen ThM. Multiple Rayleigh scattering of electromagnetic waves. J Phys I (France) 1997;7:445–83.
[52] Mackowski DW. A simplified model to predict the effects of aggregation on the absorption properties of soot particles. J Quant Spectrosc Radiat Transfer 2006;100:237–49.
[53] Mackowski DW. Calculation of total cross sections of multiple-sphere clusters. J Opt Soc Am A 1994;11:2851–61.
[54] Mishchenko MI, Mackowski DW. Light scattering by randomly oriented bispheres. Opt Lett 1994;19:1604–6.
[55] Mackowski DW, Mishchenko MI. Calculation of the *T* matrix and the scattering matrix for ensembles of spheres. J Opt Soc Am A 1996;13:2266–78.
[56] Mishchenko MI, Travis LD, Lacis AA. In: Scattering, absorption, and emission of light by small particles. Cambridge: Cambridge U. Press; 2002.
[57] Mackowski DW, 〈ftp://ftp.eng.auburn.edu/pub/dmckwski/scatcodes/index.html〉.
[58] Hovenier JW, van der Mie C, Domke H. In: Transfer of polarized light in planetary atmospheres—basic concepts and practical methods. Dordrecht: Kluwer; 2004.
[59] Van de Hulst HC. In: Light scattering by small particles. New York: Wiley; 1957.
[60] Tsang L, Kong JA, Shin RT. In: Theory of microwave remote sensing. New York: Wiley; 1985.
[61] Stephens GL. In: Remote sensing of the lower atmosphere. New York: Oxford U. Press; 1994.
[62] Lenke R, Maret G. Multiple scattering of light: coherent backscattering and transmission. In: Brown W, Mortensen K, editors. Scattering in polymeric and colloidal systems. Amsterdam: Gordon and Breach; 2000. p. 1–73.
[63] Videen G, Kocifaj M, editors. Optics of cosmic dust. Dordrecht, The Netherlands: Kluwer; 2002.
[64] van Tiggelen BA, Skipetrov SE, editors. Wave scattering in complex media: from theory to applications. Dordrecht, The Netherlands: Kluwer; 2003.
[65] Videen G, Yatskiv YS, Mishchenko MI, editors. Photopolarimetry in remote sensing. Dordrecht, The Netherlands: Kluwer; 2004.
[66] Tuchin VV, Wang LV, Zimnyakov DA. In: Optical polarization in biomedical applications. Berlin: Springer; 2006.
[67] Hansen JE, Travis LD. Light scattering in planetary atmospheres. Space Sci Rev 1974;16:527–610.
[68] Mishchenko MI, Travis LD. Light scattering by polydisperse, rotationally symmetric nonspherical particles: linear polarization. J Quant Spectrosc Radiat Transfer 1994;51:759–78.
[69] Etemad S, Thompson R, Andrejko MJ, et al. Weak localization of photons: termination of coherent random walks by absorption and confined geometry. Phys Rev Lett 1987;59:1420–3.
[70] Petrova EV, Tishkovets VP, Jockers K. Modeling of opposition effects with ensembles of clusters: interplay of various scattering mechanisms. Icarus 2007;188:233–45.
[71] Tishkovets VP. Light scattering by closely packed clusters: shielding of particles by each other in the near field. J Quant Spectrosc Radiat Transfer 2008;109:2665–72.